

High-gradient two-beam accelerator structure

S. Yu Kazakov,^{1,2} S. V. Kuzikov,^{1,3} Y. Jiang,⁴ and J. L. Hirshfield^{1,4,*}

¹*Omega-P, Inc., 258 Bradley Street, New Haven, Connecticut 06510, USA*

²*High Energy Accelerator Research Organization KEK, 1-1 Oho, Tsukuba, Ibaraki, 305-0801, Japan*

³*Institute of Applied Physics, Russian Academy of Sciences, 46 Ulyanov Street, Nizhny Novgorod, 603950, Russia*

⁴*Physics Department, Yale University, New Haven, Connecticut 06520-8120, USA*

(Received 9 March 2010; published 26 July 2010)

A novel cavity structure is described that could be the basis for a two-beam, high-gradient, accelerator. Versions of the structure could be used for acceleration of beams of electrons, positrons, muons, protons, or heavier ions; with either electron or proton drive beams. The structure embodies cavities that are excited in several harmonically related eigenmodes, such that rf fields reach their peak values only during small portions of each basic rf period. This feature could help raise breakdown and pulse heating thresholds. The two-beam accelerator structure comprises chains of these cavities. In this configuration, no transfer elements are needed to couple rf energy from the drive beam to the accelerated beam, since both beams traverse the same cavities. Purposeful cavity detuning is used to provide much smaller deceleration for a high-current drive beam, than acceleration for a low-current accelerated beam, i.e., to provide a high transformer ratio. A self-consistent theory is presented to calculate idealized acceleration gradient, transformer ratio, and efficiency for energy transfer from the drive beam to the accelerated beam, for either parallel or antiparallel motion of the beams. The theory has been cast in dimensionless quantities so as to facilitate optimization with respect to efficiency, acceleration gradient, or transformer ratio, and to illuminate the interdependence of these parameters. Means for dramatically shortening the structure fill time are also described. However, no beam dynamics analysis is presented, so the range of parameters within which this new acceleration concept can be used will remain uncertain until it is established that stable beam transport along the structure using an appropriate focusing system is possible.

DOI: 10.1103/PhysRevSTAB.13.071303

PACS numbers: 29.20.Ej, 84.40.-x, 28.65.+a

I. INTRODUCTION

Great interest attaches to any new concept that could lead to practical design of a high-gradient linear accelerator for a future multi-TeV electron-positron collider, for an efficient proton driver, or for a compact medical accelerator. This paper describes a new type of rf cavity structure for a two-beam accelerator [1], with cavities that are excited by a drive beam in several harmonically related modes that are detuned from resonance to allow achievement of a high transformer ratio [2,3]. As will be shown below, this two-beam structure embodies a number of other appealing features, namely (a) the structure is all metallic; (b) no transfer or coupling elements are needed between the drive and acceleration channels; (c) the cavity fields are symmetric with respect to the paths of the drive beam and the accelerated beam; and (d) exposure times for the peak rf electric and magnetic fields on cavity surfaces are less than for a single-mode cavity at the same fundamental frequency with the same pulse width. Features (a) and (b) lead to simplicity in construction and savings in cost. Feature (c) is favorable from a beam stability standpoint. Feature (d) could allow rf breakdown and pulse heating

thresholds to be higher than for a conventional cavity that operates at the same fundamental frequency. Finally, a high transformer ratio can make the structure attractive for a two-beam accelerator, since this leads to fewer drive beam stages than for an interaction with low transformer ratio.

Other two-beam accelerator systems have been described [4] and one, CLIC at CERN [5], is under intense study. Another, based on dielectric wakefields generated in cylindrical cross-section structures [6,7], has been tested. Also, two-beam accelerator configurations with structures built of rectangular or coaxial cross-section dielectric-lined elements are under development [8,9].

In a collinear two-beam accelerator, decelerated drive bunches and accelerated test bunches travel along the same channel. Usually, in this arrangement, particles in a test bunch can acquire energy at a rate that cannot exceed about twice the average energy loss of particles in a drive bunch; this is often expressed through the transformer ratio \mathcal{T} which, according to Wilson's theorem [10], will normally not exceed a value of 2. The number of drive beam sections N in a two-beam accelerator needs to be greater than $N_{\min} = W_F/\mathcal{T}W_D$, where W_F is the final beam energy and W_D is the drive beam energy. As an example, for $W_F = 1.5$ TeV, $W_D = 2.0$ GeV, and $\mathcal{T} = 2$, this translates to $N > N_{\min} = 375$, a sizable number of independent drive beam sections. It would seem that \mathcal{T} values well in excess

*Corresponding author.
jay.hirshfield@yale.edu

of 2 are desirable for a practical two-beam accelerator. In this paper, it will be shown that use of detuned cavities allows one to achieve $\mathcal{T} \gg 2$.

II. SUPERPOSITION OF HARMONICALLY RELATED CAVITY MODES

A particle beam to be accelerated is modeled in this paper to be a periodic sequence of tight bunches that move along a straight path with a velocity close to the speed of light. High accelerating fields need exist only during the narrow time intervals when test bunches traverse the cavities that comprise the accelerator structure. During time intervals between bunches, fields in each cavity should preferably be as small as possible. In each cavity, fields localized in space should move between the structure axis when a bunch to be accelerated arrives, and at other times move away from the axis and generally weaken [11,12]. This scenario is illustrated in cartoon form in Fig. 1. The rf power that flows in the longitudinal direction is neglected due to assumed small cutoff apertures between cavities only large enough for beam transport. The ideal electric field seen by bunches along the structure is sketched in Fig. 2 (curve 1—in green), in comparison with field behavior in a single-frequency structure (curve 2—in red). In the case of a limited number of modes used in the proposed accelerating structure the resulted field would look like that in curve 3—in blue.

It is widely accepted that thresholds increase for rf breakdown and thermal fatigue due to pulse heating, as one decreases the rf pulse width—or perhaps more accurately, reduces the exposure time to intense rf. It is thus natural to anticipate that a cavity in which the peak fields are present only during transit of the bunches—rather than during a substantial fraction of the interbunch period—should be capable of sustaining higher peak fields than would be the case for a cavity driven at a single frequency. This is a key feature that motivates design of cavities for an accelerator structure that support strong fields only during

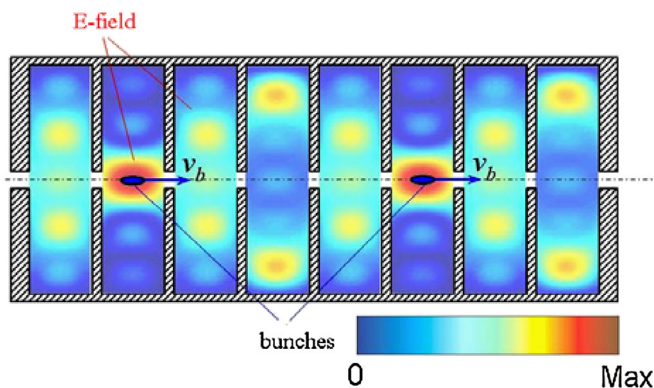


FIG. 1. (Color) Acceleration of moving periodic bunches in uncoupled cavities operating with a superposition of synchronized harmonically related eigenmodes.

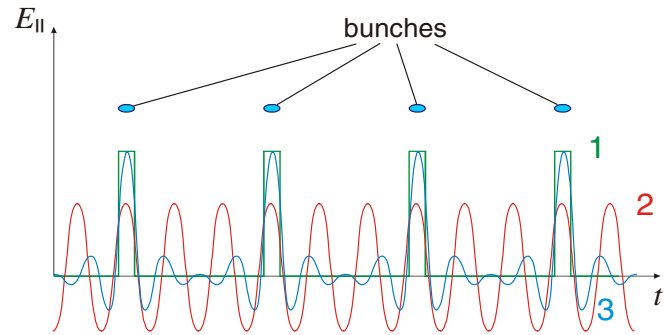


FIG. 2. (Color) Time dependence of fields in an accelerating structure consisting of a chain of uncoupled, multimode, harmonically related eigenmodes. Curve 1 (green) has the ideal time dependence; curve 2 (red) has the sinusoidal time dependence as in conventional single-frequency accelerating structures; curve 3 (blue) represents the field in a multifrequency accelerating structure operating in a limited number of modes.

a small fraction of each rf period. It is not within the scope of this paper to examine the physics underlying rf breakdown and/or pulse heating dependence upon exposure time, other than to observe that shortening the exposure time is expected to be beneficial.

The simplest structure that can produce fields such as shown in Fig. 2 is a cavity whose eigenmodes have harmonically related eigenfrequencies ω_{mn} . Thus, for the TM_{mn0} mode in a square box of side L , one has $(\omega_{mn}L/\pi c)^2 = n^2 + m^2$. Here, c is the speed of light and (m, n) are indices for transverse (x, y) field variations; the fields are uniform in the longitudinal z direction. When $n = m$, one has $\omega_{mn} = \sqrt{2}n\pi c/L$, so this class of modes has eigenfrequencies that are harmonically related. If the desired modes are to have electric fields that peak at the center of the cavity, even values of n should not be excited. However, selective external excitation of this class of modes, and no others, could prove daunting; it would require a separate phase-locked high-power source at the appropriate frequency for each mode, plus an intricate coupling scheme. Fortunately, excitation of only the odd-harmonic modes can be effectively accomplished using a drive beam consisting of a train of charge bunches injected at the frequency $\omega_{11} = \sqrt{2}\pi c/L$ along the axis of the cavity. This phenomenon is illustrated in Fig. 3, which shows the rf electric field distribution in a square box cavity excited in the three modes with frequencies ω_{11} , $\omega_{33} = 3\omega_{11}$, and $\omega_{55} = 5\omega_{11}$ due to the passage of a train of point charge bunches. The field distribution is shown at the instant when the bunch passes through the cavity and $1/20$ of a period later where the peak electric field is seen to be lower than its maximum value by about a factor of 3.

A similar comparison can be made for rf magnetic fields in the cavity. Figure 4(a) shows the magnetic field profile at its peak, 90° in phase after the peak in electric field. A strong multimode superposition is seen along the cavity walls that could promote pulse heating and surface fatigue

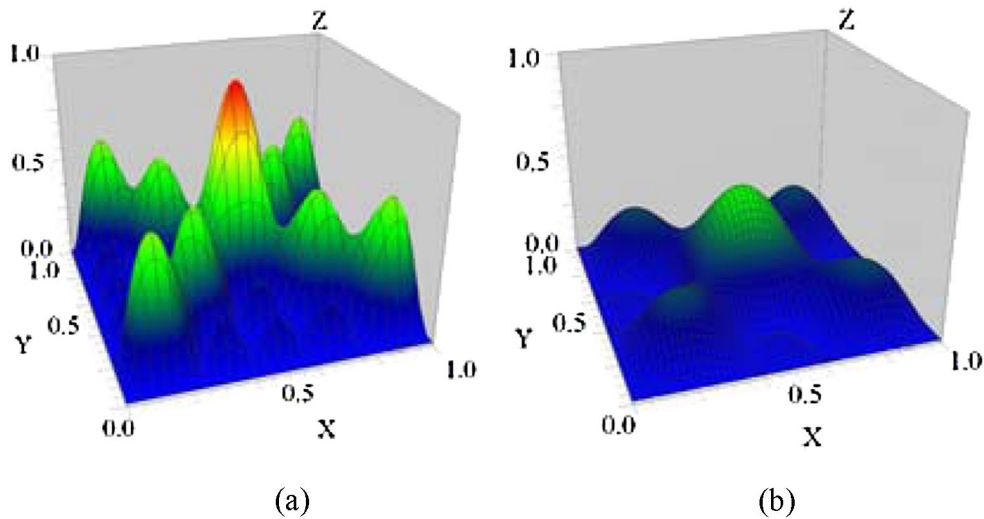


FIG. 3. (Color) (a) Axial E field in a square cavity of side L excited in its first three odd- n TM_{nm0} modes by a train of point charge bunches spaced in time by $\sqrt{2}L/c$, at the time of transit of a bunch. (b) Same as (a), except at a time $1/20$ of the bunch period after passage of the bunch. One notes that the peak electric field is now smaller by about a factor of 3, than in Fig. 3(a).

in a high-gradient cavity. Figure 4(b) shows the profile at a time $1/20$ of the bunch period after that in Fig. 4(a). As with the rf electric fields, it is seen that strong fields only persist for short portions of the bunch period.

The reduction in time of exposure to high fields that results from use of superposition of harmonic modes is illustrated in further detail in Fig. 5. Here a comparison in exposure times to the rf electric field is made between excitation in a single mode, and in three equal amplitude harmonic modes. The figure shows for the same peak fields that 95%, 90%, and 80% of the peak field is present 20%, 29%, and 41% of the time for excitation in a single mode; but these same amplitudes are only present 6%, 8.4%, and

10% of the time when three modes are excited. These exposure reductions illustrate the potential value that this strategy may hold to allow higher peak fields to be sustained before encountering unacceptable breakdown rates or excessive pulse heating.

In passing, it is worth mentioning that another rectangular structure has harmonically related modes in which both even and odd harmonics can couple to a centered beam. This structure is a rectangular box with sides L and $\sqrt{5/3}L$. Here the TM_{110} mode has eigenfrequency $\omega_{11} = \sqrt{8/5}\pi c/L$, and TM_{nm0} modes have eigenfrequencies equal to $n\omega_{11}$. But among these only the odd- n modes

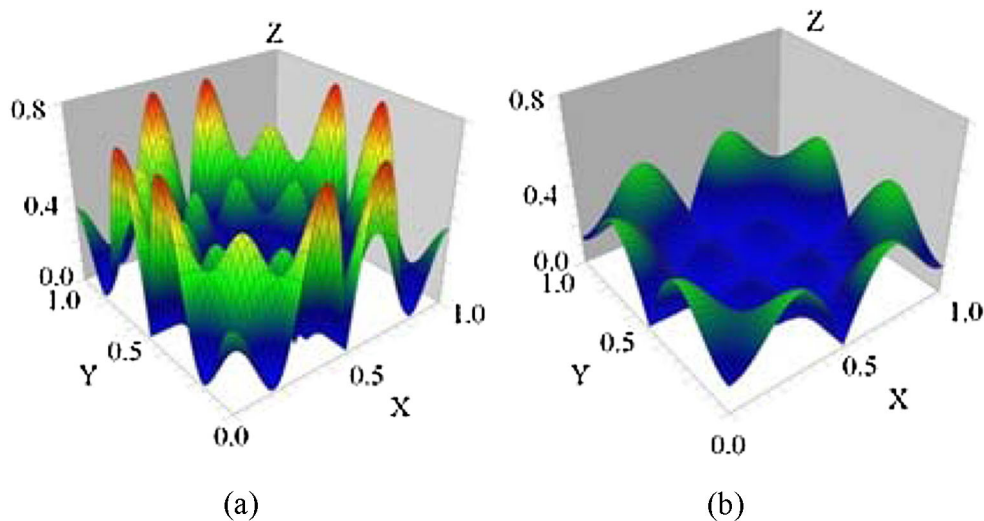


FIG. 4. (Color) (a) The rf magnetic field pattern one-quarter period after the electric field pattern shown in Fig. 3(a) appears. Note strong fields along the cavity walls. (b) The rf magnetic field pattern at a time $1/20$ of the bunch period later. The peak magnetic field on the walls is smaller by about a factor of 2, than in (a).

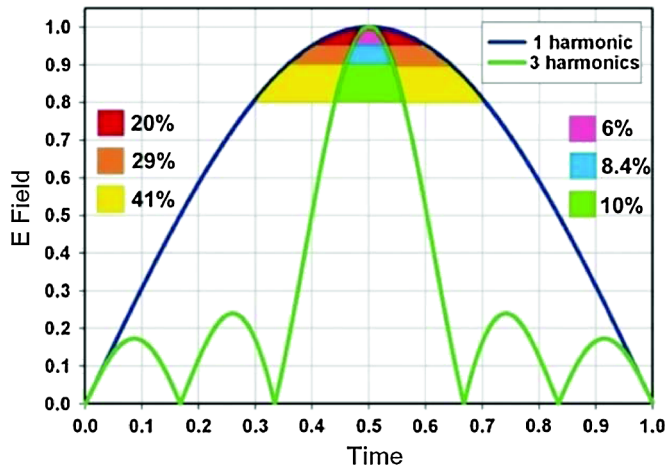


FIG. 5. (Color) Time dependence of fields in a square box cavity excited in a single mode during half of a fundamental mode period, as compared with the same cavity excited in three harmonic modes. A dramatic reduction in exposure time to strong fields for the latter case is evident. Reduction is doubled for a full cycle (cf. Fig. 2).

will couple to a centered beam, as with the square box cavity. However, it is possible to show that the $TM_{1,3,0}$, $TM_{5,1,0}$, $TM_{3,9,0}$, $TM_{1,13,0}$, and $TM_{5,15,0}$ modes have resonances at $2\omega_{11}$, $4\omega_{11}$, $6\omega_{11}$, $8\omega_{11}$, and $10\omega_{11}$, respectively, and will also couple to a centered beam. This cavity may be further superior to the square box cavity because of its more dilute density of possible spurious modes.

However, from the practical point of view, an axisymmetric cavity is preferable to a rectangular one, in order to maximize the Q factor, and to facilitate fabrication and tuning. A design for such a cavity has been found, where the first three axisymmetric modes are related harmonically. This cavity is a modified cylindrical pillbox, with the usual planar end walls tilted to obtain the harmonicity. Outline images and a drawing for this type of cavity are shown in Fig. 6. Field maps are shown in Fig. 7.

The mode eigenfrequencies and Q factors found for the first three axisymmetric modes of a copper version of this cavity (similar to TM_{010} , TM_{020} , and TM_{030} modes for a standard pillbox) are 2.999 98 GHz, 7.041×10^3 ; 5.999 95 GHz, 1.079×10^4 ; and 8.999 93 GHz, 1.408×10^4 .

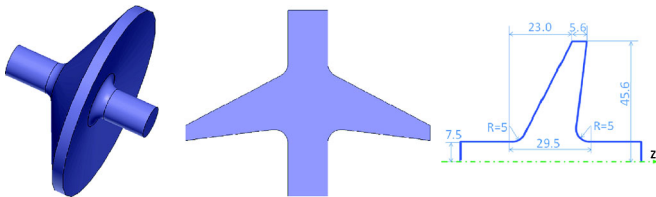


FIG. 6. (Color) Profiles and outline drawing for a modified pillbox cavity with harmonically related eigenmodes for its first three axisymmetric TM modes. Dimensions are in mm.

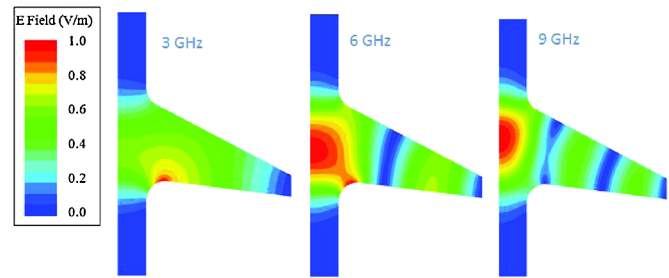


FIG. 7. (Color) Profiles, outline drawing, and field maps for an axisymmetric modified pillbox cavity with harmonically related eigenfrequencies for its first three axisymmetric modes.

It is, of course, advantageous to operate without the need to skip modes with even indices as is the case here, since this lowers the frequencies for modes above the first and thus avoids the smaller transit-time reduction factors entailed for higher mode frequencies, and lowers the number of possible spurious modes. In what follows, it is assumed that a chain of cavities similar to those shown in Figs. 6 and 7 is assembled to constitute each accelerator section.

III. A CHAIN OF DETUNED, DECOUPLED CAVITIES AS A TWO-BEAM ACCELERATOR STRUCTURE

The use of *detuned* cavities to constitute a two-beam accelerator with high transformer ratio was first introduced by Kazakov *et al.* [1]. That concept can embody excitation of several modes in a cavity as described above for raising breakdown thresholds, but is equally valid for single-mode cavities. Discussion in this section is limited to single-mode cavity excitation, but examples given below are for multimode excitation. Analysis that extends single-mode theory to multimode is given in Appendix A.

The accelerator scheme uses a drive beam having a bunch frequency detuned slightly away from the eigenfrequency for the lowest-order TM_{010} -like cylindrical cavity mode, with test bunches interspersed periodically between drive bunches. We assume that both the high-current drive beam and the low-current accelerated (or test) beam propagate collinearly along the axis of the cavity chain.

Without detuning, the electric fields induced by the decelerating drive beam particles, and in turn seen by the accelerating test particles later in the cycle, are evidently at best equal in magnitude, indicating that the transformer ratio would not exceed unity. This is clearly not a useful circumstance for a two-beam accelerator. However, the transformer ratio can be made noticeably greater than unity when the cavity is detuned. The principle of operation of a detuned cavity without loss is illustrated in Fig. 8(a), and for a cavity with loss in Fig. 8(b). Without loss, and off resonance, current and voltage for each beam are 90° out of phase with each other. Thus, the peak electric field in the cavity occurs one quarter period after passage of the drive current bunch. But, since a test particle bunch can be

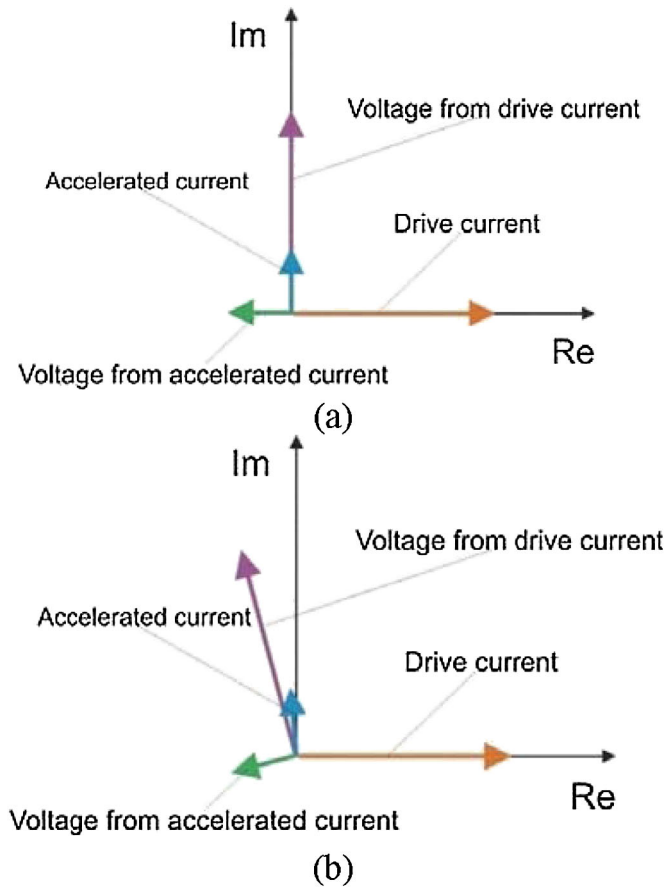


FIG. 8. (Color) (a) Exciting a detuned cavity without loss. (b) Exciting a detuned cavity with loss. Excitation off resonance allows a transformer ratio greater than unity.

phased to arrive at an arbitrary time after a drive beam bunch, drive beam voltage and accelerated (or test) beam current can be in phase (so work is done *on* the test beam particles by the drive beam), while accelerated beam voltage and drive beam current are 180° out of phase (and work is done *by* the test beam on the drive beam particles). Thus, energy is gained by the test beam, with an equal energy lost by the drive beam; and with a transformer ratio \mathcal{T} equal to the ratio of currents, i.e., $\mathcal{T} = I_D/I_T$ as in any ideal transformer. If the drive beam current were to greatly exceed the test beam current, one can view the cavity as a simple resonant circuit driven from a constant current source, where the phase lag or lead between current and voltage is zero when the bunch frequency for the drive beam current is exactly resonant with the natural frequency of the circuit. But off resonance, the voltage will lag or lead the current, depending upon the degree and sign of detuning. This differs from the customary situation with accelerator cavities driven at resonance, where the induced cavity voltage has a phase to give maximum deceleration, linked to the arrival phase of bunches in the gap. When the test beam current is not negligible, and when one seeks a self-consistent description, it is necessary to consider both

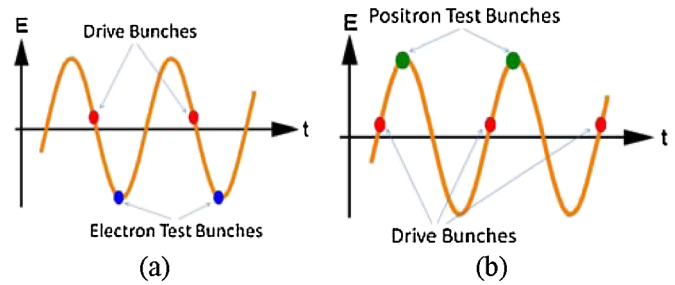


FIG. 9. (Color) (a) Accelerating test electron bunches (blue dots) and decelerating electron drive bunches (red dots). (b) Accelerating test positron bunches (green dots), and decelerating electron drive bunches (red dots), for a structure consisting of a chain of detuned cavities.

currents as comprising a “source” that induces a net gap voltage which is a phasor sum of voltages seen by both beams. Clearly, the phase differences depend upon the degree of detuning, but one is free to impose an optimum difference by adjusting the detuning. This is the premise invoked in the theory described here.

Figure 9 shows another explanation of the working of a detuned cavity, where deceleration of drive particles is seen to be much smaller (in magnitude) than is acceleration of test particles, effected solely by the relative phase angle between accelerated test bunches and decelerated drive bunches. Figure 9(a) shows the respective phases for electron acceleration, while Fig. 9(b) is for positrons. This principle of two-beam acceleration using detuned cavities does not depend on the mass of either beam species, allowing one to also consider this mechanism for two-beam acceleration of protons, muons, or heavier ions, using either an electron or proton drive beam.

IV. ANALYTIC THEORY FOR TWO-BEAM ACCELERATION IN A DETUNED CAVITY STRUCTURE

In this section, a self-consistent theory is presented for two-beam acceleration in a structure consisting of a chain of detuned cavities. For simplicity, the magnitude of detuning is assumed to be identical for all cavities. However, for some applications it turns out to be advantageous to employ detuning of alternate signs in alternate cavities; in what follows these two choices are distinguished by the labels “fixed detuning” and “alternate detuning.” The model employed has drive bunches and test bunches injected at the same frequency, so that test bunches are uniformly interleaved between drive bunches; generalization to the case of harmonically related bunch and test frequencies is straightforward. For the derivations in this section, it is assumed in the interest of clarity that only one cavity mode is excited by the drive beam. However, as described above, it could be desirable to operate with multimode excitation to reduce the exposure times of

cavity surfaces to high fields.¹ Self-consistent theory for multimode excitation is presented in Appendix A. Examples presented below are based on multimode excitation.

The test beam with current $I_T(z, t)$ is taken to propagate along the \hat{z} direction passing on axis through each cavity. The drive beam with current $I_D(z, t)$ is taken to propagate either forward along the \hat{z} direction or backward along the $-\hat{z}$ direction, also on axis. The two currents can be written as superpositions of harmonically related modal currents with frequencies ω_s and wave numbers k_{Ts} and k_{Ds} i.e.,

$$I_T(z, t) = \sum_s I_{Ts} e^{i(\omega_s t - k_{Ts} z + \phi_{Ts})} \quad (1)$$

and

$$I_D(z, t) = \sum_s I_{Ds} e^{i[\omega_s t - k_{Ds}(z - z_0) + \phi_{Ds}]}, \quad (2)$$

where ϕ_{Ds} and ϕ_{Ts} are the initial temporal phases of the modes; the wave numbers are $k_{Ts} = \omega_s/c\beta_T$ and $k_{Ds} = \omega_s/c\beta_D$ for normalized particle velocities β_T and β_D ; all quantities are positive, except that the sign of k_{Ds} goes with the sign of β_D ; and z_0 is the separation between drive and test bunches. Invoking the orthogonality of cavity eigenmodes allows decomposition of the excited electric field into independent modal components E_{zs} excited by each mode of the composite current. For purely axial currents, the excited spectrum is taken to be composed only of TM_{0m0}-like modes in a modified pillbox cavity with harmonically related eigenfrequencies (as described above). Thus the amplitude of E_{zs} is assumed to be constant along the axis within each cavity. The steady-state excited electric field in the n th cavity along the accelerator structure can be written in a Fourier series, i.e.,

$$E_z(z, t) = \sum_s E_s(z) e^{i\omega_s t} \quad (3)$$

with

$$E_s(z) = \frac{r_s}{2g^2} \frac{1}{1 + i2Q_s\delta_n} \int_{n\Lambda - g/2}^{n\Lambda + g/2} I(z) dz \quad (4)$$

as follows from a lumped-circuit model for a current-driven resonator. Thus we have

$$E(z) = \frac{r}{2g} \frac{\Theta_D I_D}{\sqrt{1 + 4Q^2\delta^2}} \times e^{-i\theta_n} \{s e^{-i(nk_T\Lambda + \phi_T)} + e^{-i[k_D(n\Lambda - z_0) + \phi_D]}\}. \quad (5)$$

¹Recently [13], it has been shown that multimode operation of a longitudinally asymmetric cylindrical cavity can result in electric fields directed towards one cavity surface that are weaker than those directed away from the opposite surface. This could result in an elevation in the rf breakdown threshold for a structure composed of such cavities, as compared with use of symmetric cavities, by analogy with breakdown in a DC vacuum diode which originates preferentially at the cathode.

In Eq. (5), the subscript s has been suppressed to simplify the notation; r_s and Q_s are the shunt impedance and quality factor of the s th cavity mode; $I(z) e^{i\omega_s t} = I_{Ds}(z, t) + I_{Ts}(z, t)$ is the s th modal component of the total beam current; g is the cavity gap and Λ is the spacing between cavity centers, both assumed to be the same for all cavities; $\delta = \Delta\omega/\omega$ is the magnitude of relative detuning, also assumed to be the same for all cavities; $\delta_n = (-1)^{\zeta n} \delta$ includes the sign of detuning, with $\zeta = 0$ for fixed detuning and $\zeta = 1$ for alternate detuning; the phase angle between current and electric field is $\theta_n = \arctan 2Q\delta_n$; $s = I_T\Theta_T/I_D\Theta_D$ is the modified current ratio; and the transit-time reduction factors are $\Theta_{D,T} = \sin(\omega_s g/2c\beta_{D,T})/(\omega_s g/2c\beta_{D,T})$.

We can now find the propagator Π_E , namely, the factor that projects the electric field from one cavity into the next. Thus, between adjacent cavities $n = 0$ and $n = 1$, we have

$$\Pi_E \equiv \frac{E_z(z = \Lambda)}{E_z(z = 0)} = \frac{s e^{-ik_T\Lambda + i\phi_T} + e^{-ik_D(\Lambda - z_0) + i\phi_D}}{s e^{i\phi_T} + e^{ik_D(z_0 + \phi_D)}} e^{i2\zeta\theta}, \quad (6)$$

where $\theta = \arctan 2Q\delta$.

The propagator for particles in the test beam is $\Pi_T = I_T(\Lambda)/I_T(0) = e^{-ik_T\Lambda}$. For phase synchronism between test particles and the accelerating field, it is necessary that the ratio Π_T/Π_E be a real number R . Thus,

$$R = e^{-i2\zeta\theta} \frac{s e^{i\phi_T} + e^{ik_D(z_0 + \phi_D)}}{s e^{i\phi_T} + e^{i(k_D z_0 + \phi_D)} e^{i(k_T - k_D)\Lambda}} \quad (7)$$

with the requirement for a vanishing imaginary part, i.e., $\Im(R) = 0$.

At this stage in the analysis we can examine four general cases, namely, parallel and antiparallel propagation of the drive and test beams, and fixed and alternate detuning of the cavities. For fixed detuning $\zeta = 0$, we find for $\Im(R) = 0$ that $(k_T - k_D)\Lambda = 2m\pi$, where m is either zero or an integer. Substituting $k_T = \omega/c\beta_T$ and $k_D = \omega/c\beta_D$ leads to the following expression that must be satisfied to ensure synchronism for fixed detuning:

$$\beta_T = \frac{\beta_D}{1 + \frac{2m\pi c\beta_D}{\omega\Lambda}}. \quad (8)$$

For alternate detuning $\zeta = 1$, the condition $\Im(R) = 0$ leads to a tangled implicit relationship between β_T and β_D that does not yield to easy interpretation. But in the limit as the modified current ratio $s \rightarrow 0$, i.e., for a test beam current much smaller than the drive beam current, we find as a condition for $\Im(R) = 0$ the equation

$$(k_D - k_T)\Lambda - 2\theta = \frac{\Lambda\omega}{c\beta_D} \left(1 - \frac{\beta_D}{\beta_T}\right) - 2\theta = 2m\pi \quad (9)$$

which gives

$$\beta_T = \frac{\beta_D}{1 - (m + \frac{\theta}{\pi}) \frac{2\pi c \beta_D}{\omega \Lambda}}. \quad (10)$$

The two equations found above that prescribe the synchronism conditions for the four cases yield fairly straightforward guidelines for the architecture of two-beam accelerators for use in various parameter regimes. For specificity in analyzing the synchronism conditions, it is assumed that $\beta_T > 0$, but that one may have either $\beta_D > 0$ (parallel beams) or $\beta_D < 0$ (antiparallel beams).

With fixed detuning and acceleration of highly relativistic particles ($\beta_T \approx 1$) using a highly relativistic drive beam ($|\beta_D| \approx 1$), it is seen from Eq. (8) for the $m = 0$ case that synchronism can be maintained with only parallel beams for arbitrary values of $2\pi c/\omega \Lambda = \lambda/\Lambda$ where the wavelength λ is the bunch spacing. For $m = 1$, synchronism requires $\Lambda \approx \lambda/2$, but for antiparallel beams only. However, the restriction $\Lambda \approx \lambda/2$ could result in either a significant transit-time field reduction or a high degree of dilution (i.e., gap g comparatively smaller than the cavity spacing Λ).

Synchronous acceleration of moderately relativistic particles ($\beta_T \leq 1$) with a highly relativistic drive beam ($|\beta_D| \approx 1$) is seen to be possible with fixed detuning and parallel beams for $m \geq 1$. However, this would require $\Lambda \ll \lambda$ for small values of β_T , which in turn would lead to relatively low energy gain for test particles crossing each gap, and a larger number of cavities with attendant greater complexity. A similar situation arises with fixed detuning and antiparallel beams for achieving synchronism for small values of β_T .

As a result, the preferred configuration for two-beam acceleration of initially low- β_T particles is seen to be that with alternate detuning. In this case, with antiparallel beams $\beta_D \approx -1$, one finds from Eq. (9) that synchronism with $\theta \approx -\pi/2$ can be obtained for $\beta_T \leq 1$, for all negative m (including zero) and for values of Λ/λ that satisfy Eq. (9); but when $\theta \approx +\pi/2$ as depicted in Figs. 8 and 9, only for $m \leq -1$ and values of Λ/λ that satisfy Eq. (9). Synchronism can prevail for arbitrarily low values of β_T if Λ/λ is low enough; but if this is too low, a scheme with M cavities detuned positive followed by M detuned negative can be used—as described below. These choices can yield transit-time reduction factors Θ_T that are close to unity. As a consequence of these factors, antiparallel beams together with alternate detuned cavities are seen to be favored choices for acceleration of low- β_T particles, say protons into the GeV range; while parallel beams would be employed in exploring regimes for acceleration of electrons or positrons up into the TeV range. It can also be pointed out that the roles of test and drive beam can be interchanged, so that a low- β high-current drive beam (say a sub-GeV high-power proton beam) could in principle drive acceleration of a low-current test beam (say multi-GeV electrons or positrons) to high energies; this exotic option will not be further pursued in this paper.

The counterintuitive possibility of synchronism for antiparallel beams arises from the particular choice of gap spacing dictated once β_T and $|\beta_D|$ are specified. The fields from a continuous periodic train of drive bunches seen by test particles when they pass each gap can appear as a synchronous wave moving opposite to the drive beam, since exposure to the drive bunch fields is restricted only to designated portions of each rf cycle. The apparent reverse sense of rotation of wagon wheel spokes often seen in films is analogous.

The synchronism conditions can now be imposed upon the expression for the electric field experienced by the test beam particles and the drive beam particles. From the real part of Eq. (5), we find the field at frequency ω_s which can do work on test particles at the center of the n th cavity at $z = n\Lambda$ and at time $t = t_T = k_T n\Lambda/\omega$, to be

$$E_T(n\Lambda, t_T) = \frac{r}{2g} \frac{\Theta_D I_D}{1 + 4Q^2 \delta^2} \{ \varsigma \cos \phi_T + 2Q \delta_n \varsigma \sin \phi_T + \cos[k_D z_0 - (k_D - k_T)n\Lambda + \phi_D] + 2Q \delta_n \varsigma \sin[k_D z_0 - (k_D - k_T)n\Lambda + \phi_D] \}. \quad (11)$$

Similarly, the excited electric field that acts on drive beam particles at $t = t_D = k_D(n\Lambda - z_0)/\omega$ when the drive beam is in the center of the n th cavity at $z = n\Lambda$ is

$$E_D(n\Lambda, t_D) = \frac{r}{2g} \frac{\Theta_D I_D}{1 + 4Q^2 \delta^2} \{ \cos \phi_D + 2Q \delta_n \sin \phi_D + \varsigma \cos[k_D z_0 - (k_D - k_T)n\Lambda - \phi_T] - 2Q \delta_n \varsigma \sin[k_D z_0 - (k_D - k_T)n\Lambda - \phi_T] \}. \quad (12)$$

Equations (11) and (12) can be applied to explore a range of parameters of two-beam collinear acceleration using an ultrarelativistic electron drive beam, for acceleration of ultrarelativistic electrons, and acceleration of moderately relativistic protons.

Electron acceleration.—For ultrarelativistic electron acceleration, the drive beam and the test beam have $\beta_T \approx \beta_D \approx 1$, and the beams propagate in the same direction so $k_D \approx k_T$. The electric field contributed by both beams that acts on test beam particles is, from Eq. (11), given by

$$E_T(n\Lambda, t_T) = \frac{r}{2g} \frac{\Theta I_D}{1 + 4Q^2 \delta^2} (\varsigma + \cos k z_0 + 2Q \delta \sin k z_0), \quad (13)$$

where $k = \omega/c$, the transit-time reduction factors are $\Theta = \sin(kg/2)/(kg/2)$ equal for both test beam and drive beam, the modified current ratio ς is the current ratio I_T/I_D itself, and the initial phases are chosen to be $\phi_T = \phi_D = 0$. Similarly, the electric field that drive beam particles experience in the center of each cavity is

$$E_D(n\Lambda, t_D) = \frac{r}{2g} \frac{\Theta I_D}{1 + 4Q^2\delta^2} \times (1 + \varsigma \cos kz_0 - 2Q\delta \sin kz_0). \quad (14)$$

By choosing the proper delay between test beam and drive beam, i.e. $z_0 = (2j - 1/2)\pi/k$ with j equal to zero or an integer, one finds

$$E_T(n\Lambda, t_T) = \frac{r}{2g} \frac{\Theta I_D}{1 + 4Q^2\delta^2} (\varsigma - 2Q\delta) \quad (15)$$

and

$$E_D(n\Lambda, t_D) = \frac{r}{2g} \frac{\Theta I_D}{1 + 4Q^2\delta^2} (1 + 2Q\delta\varsigma). \quad (16)$$

So the transformer ratio $\mathcal{T} = E_T/E_D$ for ultrarelativistic two-beam electron acceleration, i.e., the ratio of accelerating field seen by the test particles to the decelerating field seen by the drive particles, is

$$\mathcal{T} = \frac{\varsigma - 2Q\delta}{1 + 2Q\delta\varsigma}. \quad (17)$$

As an example from these equations, for a drive beam current of 100.8 A and an accelerated beam current of 4.8 A, an acceleration gradient of over 150 MV/m is predicted for cavity detuning of $\Delta\omega/\omega = 0.9 \times 10^{-3}$, with a transformer ratio of 13:1 and a beam-to-beam power transfer efficiency of 60%. Here, the bunch frequency is assumed to be 3.0 GHz, the Gaussian bunch lengths to be 15 ps (4.5 mm), the cavity gap widths to be 3.65 cm, walls between cavities to be 1 mm thick, and Q values for copper are used.

Proton acceleration.—For proton acceleration, the drive beam is relativistic with $\beta_D \approx -1$, while the test beam has $\beta_T \leq 1$ and propagates in the opposite direction. The cavity chain has alternatively detuned cavities, tuned equally above and below the drive beam frequency. By choosing the proper delay between test beam and drive beam, that is with $(k_D - k_T)n\Lambda - k_D z_0 = (2j - 1/2)\pi$ with j equal to zero or an integer, one finds expressions identical to those for ultrarelativistic electron acceleration, except that the transit-time reduction factors are different, and the modified current ratio ς reverts to $I_T\Theta_T/I_D\Theta_D$. Thus, for acceleration of moderately relativistic particles (say protons), one has

$$E_T(n\Lambda, t_T) = \frac{r}{2g} \frac{\Theta_D I_D}{1 + 4Q^2\delta^2} (\varsigma - 2Q\delta) \quad (18)$$

and

$$E_D(n\Lambda, t_D) = \frac{r}{2g} \frac{\Theta_D I_D}{1 + 4Q^2\delta^2} (1 + 2Q\delta\varsigma). \quad (19)$$

The transformer ratio \mathcal{T} is given by the same relationship as for ultrarelativistic electrons. It should be noted that the mass of the accelerated species does not enter into any of

these equations, so they could apply to moderately relativistic muons or heavy ions, as well as to protons.

As an example predicted by these equations for a 1-GeV proton accelerator, the electron drive current is taken to be 25.2 A and the proton accelerated current to be 2.4 A, giving a proton pulsed power of 2.4 GW; a duty factor of 4.2×10^{-3} would give an average beam power of 10 MW. The bunch frequency is 3.0 GHz, and the Gaussian bunches are 15 ps long. In one case, the cavity frequencies are alternately detuned with $\Delta\omega/\omega = \pm 6 \times 10^{-4}$, giving $\mathcal{T} \approx 4.5$, so the drive beam energy would be ~ 225 MeV; the average acceleration gradient is predicted to be ~ 100 MV/m. The drive bunches are 8.4 nC each while the proton bunches are 0.8 nC each, i.e., 5×10^9 protons/bunch. The accelerator structure has gradually increasing cavity and gap widths. Walls between adjacent cavities are taken to be 1 mm thick and Q values for copper are used. In contrast, for alternate cavity detunings of $\Delta\omega/\omega = \pm 3 \times 10^{-3}$, one finds $\mathcal{T} \approx 9.0$, so the drive beam energy would be about 110 MeV. Here, the average acceleration gradient is about 20 MV/m. These examples show the inherent trade-off between transformer ratio and acceleration gradient that can be encountered, in this case merely by changing the detuning.

Power transfer.—The power transfer ΔP from a beam into the cavity is given by $\Delta P = \Re \int dz I^* \cdot E/2$, where \Re signifies the real part of the quantity that follows. Hence, the power gain of the test beam in the n th cavity is

$$\begin{aligned} \Delta P_T^{(n)} &= -\Re \int_{n\Lambda-g/2}^{n\Lambda+g/2} dz I_T^* \cdot E_T/2 \\ &= -\frac{I_D^2 r \Theta_D^2}{4(1 + 4Q^2\delta^2)} \\ &\quad \times \{\varsigma^2 + \varsigma \cos[k_D z_0 - (k_D - k_T)n\Lambda + \phi_D - \phi_T] \\ &\quad + 2Q\delta_n \varsigma \sin[k_D z_0 - (k_D - k_T)n\Lambda + \phi_D - \phi_T]\}. \end{aligned} \quad (20)$$

A minus sign is explicitly added in the first line to anticipate positive power gain by the test beam from the cavity. Similarly, the power loss of the drive beam into the n th cavity is

$$\begin{aligned} \Delta P_D^{(n)} &= \Re \int_{n\Lambda-g/2}^{n\Lambda+g/2} dz I_D^* E_D/2 \\ &= \frac{I_D^2 r \Theta_D^2}{4(1 + 4Q^2\delta^2)} \{1 + \varsigma \cos[k_D z_0 - (k_D - k_T)n\Lambda \\ &\quad + \phi_D - \phi_T] - 2Q\delta_n \varsigma \sin[k_D z_0 - (k_D - k_T)n\Lambda \\ &\quad + \phi_D - \phi_T]\}. \end{aligned} \quad (21)$$

The power dissipated in the walls of the n th cavity is

$$\begin{aligned}\Delta P_W^{(n)} &= V^2/r \\ &= \frac{I_D^2 r \Theta_D^2}{4(1 + 4Q^2 \delta^2)} \\ &\quad \times \{1 + \varsigma^2 + 2\varsigma \cos[k_D z_0 - (k_D - k_T)n\Lambda \\ &\quad + \phi_D - \phi_T]\},\end{aligned}\quad (22)$$

where $V = gE$ is the amplitude of the voltage across the cavity gap. One can verify the self-consistency of this model by checking energy conservation, namely $\Delta P_D^{(n)} = \Delta P_T^{(n)} + \Delta P_W^{(n)}$, which confirms that the equations correctly show that power taken from the drive beam is completely accounted for by wall losses and power gain of the test beam.

Power transfer for electron acceleration.—The power transfer equations in the two-beam structure for electron acceleration can be written as

$$\Delta P_T = I_D^2 r \Theta_D^2 \frac{-\varsigma^2 - \varsigma(2Q\delta \sin\psi + \cos\psi)}{4(1 + 4Q^2 \delta^2)} \quad (23)$$

$$\Delta P_D = I_D^2 r \Theta_D^2 \frac{1 + \varsigma(-2Q\delta \sin\psi + \cos\psi)}{4(1 + 4Q^2 \delta^2)} \quad (24)$$

$$\Delta P_W = I_D^2 r \Theta_D^2 \frac{1 + \varsigma^2 + 2\varsigma \cos\psi}{4(1 + 4Q^2 \delta^2)}, \quad (25)$$

where the initial phase difference is $\psi = k_D z_0 + \phi_D - \phi_T$. One can maximize the test beam power gain ΔP_T by choosing the initial phase $\psi = -\arctan 2Q\delta$ and applying the synchronization condition [Eq. (8)]. In the limit $Q\delta \gg 1$, one can simplify the expression by approximating $\psi = -\pi/2$, to yield

$$\Delta P_T = \frac{I_D^2 r \Theta_D^2}{4} \frac{2Q\delta\varsigma - \varsigma^2}{1 + 4Q^2 \delta^2} \quad (26)$$

$$\Delta P_D = \frac{I_D^2 r \Theta_D^2}{4} \frac{2Q\delta\varsigma + 1}{1 + 4Q^2 \delta^2}. \quad (27)$$

Power transfer for proton acceleration.—For the proton accelerator case, we have considered a cavity chain with alternative $+M - M$ cavity detunings, i.e., with M cavities having positive detuning followed by M cavities having negative detuning, etc. The time-averaged power gain of the test beam per cavity is found to be

$$\begin{aligned}\Delta P_T &= \frac{1}{2M} \sum_{n=0}^{2M-1} \Delta P_T^{(n)} \\ &= -\frac{I_D^2 r \Theta_D^2 \varsigma}{4M(1 + 4Q^2 \delta^2)} \left\{ M\varsigma + (2Q\delta \sin\Psi + \cos\Psi) \right. \\ &\quad \left. \times \cos[\psi - (2M - 1)\Psi] \frac{\sin(2M\Psi)}{\sin(2\Psi)} \right\},\end{aligned}\quad (28)$$

where $\Psi = (k_D - k_T)\Lambda/2$ and $\psi = k_D z_0 + \phi_D - \phi_T$. Similarly, the power loss of the drive beam can be shown to be

$$\begin{aligned}\Delta P_D &= \frac{I_D^2 r \Theta_D^2}{4M(1 + 4Q^2 \delta^2)} \left\{ M + \varsigma(-2Q\delta \sin\Psi + \cos\Psi) \right. \\ &\quad \left. \times \cos[\psi - (2M - 1)\Psi] \frac{\sin(2M\Psi)}{\sin(2\Psi)} \right\},\end{aligned}\quad (29)$$

Particularly for the case of $M = 1$ with $\beta_T < 1$, the power gain of the test beam is

$$\begin{aligned}\Delta P_T &= -\frac{I_D^2 r \Theta_D^2 \varsigma}{4(1 + 4Q^2 \delta^2)} [\varsigma + (2Q\delta \sin\Psi + \cos\Psi) \\ &\quad \times \cos(\psi - \Psi)]\end{aligned}\quad (30)$$

and the power loss of the drive beam is

$$\begin{aligned}\Delta P_D &= \frac{I_D^2 r \Theta_D^2 \varsigma}{4(1 + 4Q^2 \delta^2)} [1 + \varsigma(-2Q\delta \sin\Psi + \cos\Psi) \\ &\quad \times \cos(\psi - \Psi)].\end{aligned}\quad (31)$$

By applying the synchronization condition, Eq. (9), one has $2\Psi = (k_D - k_T)\Lambda = 2\theta$, so for a proper choice of the phase delay between test beam and drive beam $\psi = \Psi$, in the limit $Q\delta \gg 1$, one finds

$$\Delta P_T = \frac{I_D^2 r \Theta_D^2}{4} \frac{2Q\delta\varsigma - \varsigma^2}{1 + 4Q^2 \delta^2} \quad (32)$$

$$\Delta P_D = \frac{I_D^2 r \Theta_D^2}{4} \frac{2Q\delta\varsigma + 1}{1 + 4Q^2 \delta^2}. \quad (33)$$

It is seen that these formulas are identical to those for electron acceleration, provided the full form for the modified current ratio ς is used.

Parameter space.—The theory developed above provides the interrelationships between the main parameters, as is needed to provide guidance in optimizing structure design for a particular application. The fundamental parameters are the cavity peak field amplitude E_T seen by the accelerated test particles, the power transfer efficiency η between drive and accelerated beams, and the transformer ratio \mathcal{T} . These parameters depend upon cavity detuning $\delta = \Delta\omega/\omega$, cavity quality factor Q , and modified current ratio ς between the beams. It is important to note that each beam is only characterized by its current and normalized particle velocity β , and not explicitly by the beam energy or beam particle mass.

To restate results of the previous derivations, the excited electric field Eqs. (15) and (18) that the test beam experiences at the center of cavity can be expressed as

$$E_T = \Xi \frac{2\varsigma - 4\Delta}{1 + 4\Delta^2} \quad (34)$$

while the excited electric field the drive beam experiences at the center of cavity can be expressed as

$$E_D = \Xi \frac{2 + 4\Delta\varsigma}{1 + 4\Delta^2}, \quad (35)$$

where $\Delta = \mathcal{Q}(\Delta\omega/\omega)$, and with the normalization factor for the electric field $\Xi = r\Theta_D I_D/4g$.

The power gain of the test beam can be written as

$$\Delta P_T = \frac{I_D^2 r \Theta_D^2}{4} \frac{2\Delta\varsigma - \varsigma^2}{1 + 4\Delta^2} \quad (36)$$

and the power loss of the drive beam can be written as

$$\Delta P_T = \frac{I_D^2 r \Theta_D^2}{4} \frac{2\Delta\varsigma + 1}{1 + 4\Delta^2}. \quad (37)$$

It is instructive to normalize all quantities to dimensionless variables, defined as follows.

Modified current ratio $\varsigma = (\Theta_T/\Theta_D)(I_T/I_D)$, where I_T and I_D are the test (i.e., accelerated) current and the drive current, and where Θ_T and Θ_D are the respective beam transit-time reduction factors, e.g., $\Theta_{T(D)} = \sin(\pi g/\beta_{T(D)}\lambda)/(\pi g/\beta_{T(D)}\lambda)$ with g the cavity gap width,

and λ the free-space wavelength. For the electron-electron two-beam case, $\beta = 1$.

Transformer ratio $\mathcal{T} = E_T/E_D$ is the ratio of accelerating field seen by the test particles, to the decelerating field seen by the drive particles.

Beam-to-beam power transfer efficiency $\eta = -I_T E_T \Theta_T / I_D E_D \Theta_D \equiv -\varsigma \mathcal{T}$.

Normalized detuning factor $\Delta = \mathcal{Q}(\Delta\omega/\omega)$, where \mathcal{Q} is the cavity quality factor and $(\Delta\omega/\omega)$ is the fractional frequency detuning for the cavities, fixed or alternating in sign for each successive cavity, and assumed to be equal for all modes.

Normalized electric field $\varepsilon = E_T/\Xi$. The field seen by the drive beam is $E_D = \varepsilon \Xi / \mathcal{T}$.

These five quantities can be shown to be related as follows:

$$\mathcal{T} = \frac{\varsigma - 2\Delta}{1 + 2\varsigma\Delta} \quad (38)$$

and

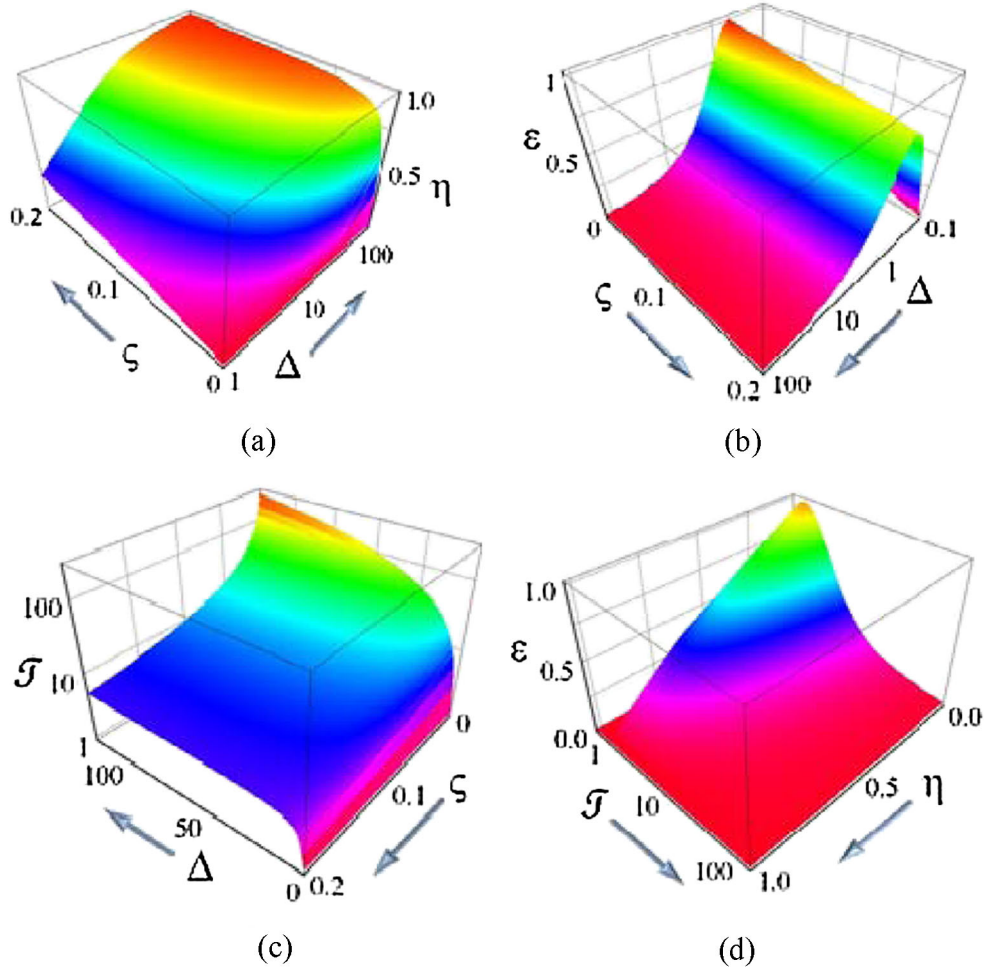


FIG. 10. (Color) Two-beam accelerator parameters. Parts (a), (b), and (c) show efficiency η , normalized accelerating gradient seen by test particles ε , and transformer ratio \mathcal{T} , each as a function of modified current ratio ς and normalized detuning Δ . Part (d) shows ε as a function of \mathcal{T} and η .

$$\varepsilon = \frac{2s - 4\Delta}{1 + 4\Delta^2} \quad (39)$$

subject to the constraints $|\varepsilon| + \eta \leq 1$, $(2\Delta - s)s > 0$, $\varepsilon(\varepsilon + 2s) \leq 1$, and $\varepsilon\Delta < 1$. These relationships show that there is a direct trade-off between efficiency and acceleration gradient. One can use any two of parameters $\{s, \varepsilon, \mathcal{T}, \Delta, \eta\}$ to represent the rest. For example, using the modified current ratio s and the scaled detuning Δ as parameters,

$$\mathcal{T} = \frac{s - 2\Delta}{2\Delta s + 1} \quad (40)$$

$$\eta = \frac{2\Delta s - s^2}{2\Delta s + 1} \quad (41)$$

$$\varepsilon = \frac{2s - 4\Delta}{1 + 4\Delta^2}. \quad (42)$$

While using the efficiency η and the transformer ratio \mathcal{T} as parameters, one has

$$\varepsilon = -\frac{2(1 - \eta)\mathcal{T}}{1 + \mathcal{T}^2}. \quad (43)$$

Graphical representations to show the interrelationships are shown in Fig. 10. Figures 10(a) and 10(b) show the strong trade-off between efficiency η and accelerating gradient ε : Fig. 10(a) shows that efficiency is high for large detuning Δ and large current ratio s ; while Fig. 10(b) shows that accelerating gradient ε peaks with the detuning factor $\Delta \approx 1$, and that it falls as the current ratio s increases. Figure 10(c) shows the transformer ratio \mathcal{T} to be a strong function of current ratio s , decreasing as current ratio increases, but that it is a weak function of detuning Δ , unless the detuning is small—in which case \mathcal{T} is also small. Figure 10(d) recasts the picture, showing again that the accelerating field ε falls as transformer ratio \mathcal{T} and efficiency η increase. These relationships provide important guidance in optimizing design.

V. CONCLUSIONS

A novel cavity structure has been described that could be the basis for a two-beam high-gradient accelerator. Versions of the structure could be used for acceleration of beams of electrons, positrons, muons, protons, or heavier ions; with either electron or proton drive beams. The structure embodies novel axisymmetric cavities that are excited in several harmonically related eigenmodes, such that rf fields reach their peak values only during small portions of each basic rf period. This feature could help raise breakdown and pulse heating thresholds. The two-beam accelerator structure comprises chains of these cavities. In this configuration, no transfer elements are needed to couple rf energy from the drive beam to the accelerated beam, since both beams traverse the same cavities.

Purposeful cavity detuning has been shown to provide much smaller deceleration for a high-current drive beam than acceleration for a low-current accelerated beam, i.e., to provide a high transformer ratio. A self-consistent theory has been presented to calculate idealized acceleration gradient, transformer ratio, and efficiency for energy transfer from the drive beam to the accelerated beam, for both parallel and antiparallel motion of the beams. The theory has been cast in dimensionless quantities so as to facilitate optimization with respect to efficiency, acceleration gradient, or transformer ratio; and to illuminate the interdependence of these parameters. Means for dramatically shortening the structure fill time are also described (see Appendix B). Preliminary examples have been provided for electron and proton accelerators, in each case using a high-current electron drive beam. However, it is important to stress that no beam dynamics analysis has yet been presented, so the range of parameters within which this new acceleration concept can be used will remain uncertain until it is established that stable beam transport along the structure using an appropriate focusing system is possible.

ACKNOWLEDGMENTS

Appreciation is extended to V.P. Yakovlev for helpful discussions. This work was supported by Office of High Energy Physics, U.S. Department of Energy.

APPENDIX A: FORMALISM FOR MULTIMODE ACCELERATOR STRUCTURE

By analogy to the single-mode excitation detailed in the body of this paper, we here develop the formalism for the multimode accelerator structure. Applying Eqs. (1) and (2) into Eq. (3), one can write the excited electric field $E_T(t) = \sum_s E_{Ts} e^{i\omega_s t}$, where the s th mode of electric field in the n th cavity is

$$E_{Ts} = \frac{r_s}{2g} \frac{I_{Ds}}{1 + i2Q_s \delta_{ns}} \times [\xi_s e^{i\phi_{Ts}} e^{-ink_{Ts}\Lambda} \Theta_{Ts} + e^{i\phi_{Ds}} e^{-ink_{Ds}(n\Lambda - z_0)} \Theta_{Ds}] \quad (A1)$$

and the transit-time factors are $\Theta_{T(D)s} = 2 \sin(k_{T(D)s}g/2)/k_{T(D)s}g$ and $\xi_s = I_{Ts}/I_{Ds}$.

The power transfer in the cavity can be written as the sum of power gain or loss of each mode ΔP_s , by taking the time average over the period of the fundamental frequency mode such that the cross terms with higher frequencies drop out,

$$\Delta P = \Re \int dz I^* \cdot E/2 = \Re \sum_s \int dz I_s^* \cdot E_s/2 = \sum_s \Delta P_s. \quad (A2)$$

Hence, the average power gain of the test beam in the n th cavity is

$$\begin{aligned} \Delta P_T^{(n)} = & - \sum_s \frac{I_{D_s}^2 r_s \Theta_{D_s}^2}{4(1 + 4Q_s^2 \delta_s^2)} \\ & \times \{ \varsigma_s^2 + \varsigma_s \cos[k_{D_s} z_0 - (k_{D_s} - k_{T_s}) n \Lambda \\ & + \phi_{D_s} - \phi_{T_s}] + 2Q_s \delta_{ns} \varsigma_s \\ & \times \sin[k_{D_s} z_0 - (k_{D_s} - k_{T_s}) n \Lambda + \phi_{D_s} - \phi_{T_s}] \}. \end{aligned} \quad (\text{A3})$$

Similarly, the average power loss of the drive beam in the n th cavity is

$$\begin{aligned} \Delta P_D^{(n)} = & \sum_s \frac{I_{D_s}^2 r_s \Theta_{D_s}^2}{4(1 + 4Q_s^2 \delta_s^2)} \\ & \times \{ 1 + \varsigma_s \cos[k_{D_s} z_0 - (k_{D_s} - k_{T_s}) n \Lambda \\ & + \phi_{D_s} - \phi_{T_s}] - 2Q_s \delta_{ns} \varsigma_s \\ & \times \sin[k_{D_s} z_0 - (k_{D_s} - k_{T_s}) n \Lambda + \phi_{D_s} - \phi_{T_s}] \}. \end{aligned} \quad (\text{A4})$$

The average power dissipated in the n th cavity wall is

$$\begin{aligned} \Delta P_W^{(n)} = & \sum_s \frac{I_{D_s}^2 r_s \Theta_{D_s}^2}{4(1 + 4Q_s^2 \delta_s^2)} \{ 1 + \varsigma_s^2 + 2\varsigma_s \\ & \times \cos[k_{D_s} z_0 - (k_{D_s} - k_{T_s}) n \Lambda + \phi_{D_s} - \phi_{T_s}] \}. \end{aligned} \quad (\text{A5})$$

These last three equations combine to satisfy the energy conservation relationship $\Delta P_{Dn} = \Delta P_{Tn} + \Delta P_{Wn}$, showing as it must that energy delivered by the drive beam is converted into wall losses and energy gain of the test beam. Following the same derivation for single mode detailed above, the interrelation between the accelerating field ε_s , transformer ratio \mathcal{T}_s , and efficiency η_s is shown to be still valid for individual modes. These relationships provide important guidance in optimizing design. The drive current profile and cavity structure will modify the contribution of each mode to the accelerating field spatially and temporally, hence effect the exposure time of the cavity to the peak field.

APPENDIX B: TRANSIENT SUPPRESSION

Excitation of detuned cavities involves a filling time, as for tuned cavities, except that (as shown below) the customary exponential buildup of cavity fields has interference beats at the detuning frequency interval superimposed upon it. Energy dissipated during cavity fill times represents an inefficiency, elimination of which would be advantageous in many applications. In this Appendix, several means are described for shortening the fill time for detuned (or even tuned) cavities—typically by 1 order of magnitude.

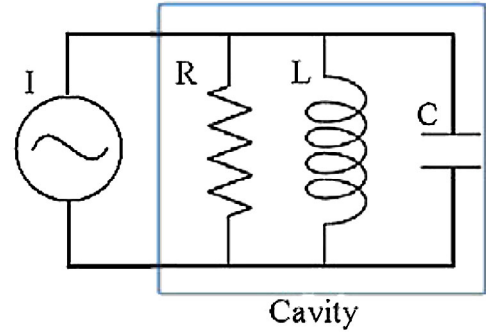


FIG. 11. (Color) Simplified equivalent circuit of the cavity driven by a current I .

A simplified model of cavity filling can be demonstrated using the equivalent lumped-parameter circuit driven by a current I as shown in Fig. 11. Any frequency shift due to beam loading is ignored here as it would typically be much smaller than the imposed detuning for the two-beam structure discussed above.

The drive current is at frequency ω , which is slightly detuned from the cavity resonance frequency $\omega_0 = \sqrt{1/LC}$. For small detuning $\Delta\omega = \omega - \omega_0$, one has $\Delta\omega/\omega \ll 1$. The differential equation describing transient buildup of voltage V is

$$\frac{V}{R} + CV\dot{V} + \frac{1}{L} \int V dt = I e^{i\omega t}. \quad (\text{B1})$$

The solution, subject to the initial conditions $V(0) = \dot{V}(0) = 0$ is

$$V = \frac{I R e^{i\omega t}}{1 + i2Q\Delta\omega/\omega} (1 - e^{-t/\tau} e^{-i\Delta\omega t}) \quad (\text{B2})$$

with the condition $Q \gg 1$ and $4Q^2 \Delta\omega/\omega \gg 1$, where the quality factor is $Q = R/\omega_0 L = RC\omega_0$ and the nominal cavity filling time $\tau = 2Q/\omega_0$. Inside the parentheses, one

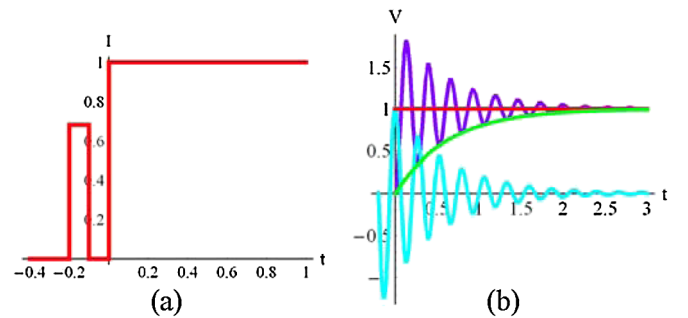


FIG. 12. (Color) Fore pulse method. (a) Current profile. (b) The reduced filling time by cancellation of the two beating transients. The cyan curve is the voltage induced by the first step pulse, the purple curve is induced by the second one, the red curve is the final voltage by summing two beating transients, and the green curve is the standard filling time curve for a single step pulse.

can see the second term is the transient term with a decay-oscillation at the beat frequency $\Delta\omega$.

To minimize transient effects, several methods can be considered that involve injecting a prepulse current prior to the main pulse. One example is shown in Fig. 12(a), in which a square pulse I_1 rises at $t = -t_1$ with pulse width T that induces a voltage V_1 , followed by a step pulse I_2 at $t = 0$, where V_1 is

$$V_1 = -\frac{I_1 R e^{i\omega t} e^{-i\Delta\omega t} e^{-t/\tau}}{1 + i2Q\Delta\omega/\omega} e^{-i\Delta\omega t_1} e^{-t_1/\tau} \times e^{i\omega t_1} (1 - e^{i\Delta\omega T} e^{T/\tau}) \quad (\text{B3})$$

which will asymptotically decay away. By summing Eqs. (B2) and (B3), the induced total voltage after $t = 0$ is

$$V(t) = \frac{R e^{i\omega t}}{1 + i2Q\Delta\omega/\omega} \{I_2 - [I_2 + I_1 e^{-i\Delta\omega t_1} e^{-t_1/\tau} \times e^{i\omega t_1} (1 - e^{i\Delta\omega T} e^{T/\tau})] e^{-i\Delta\omega t} e^{-t/\tau}\}. \quad (\text{B4})$$

By choosing $I_1 = -I_2 e^{i\Delta\omega t_1} e^{t_1/\tau} e^{-i\omega t_1} / (1 - e^{i\Delta\omega T} e^{T/\tau})$, the second term in the bracket (the beating decay component) is canceled and the total voltage immediately reaches the steady state $V = I_2 R e^{i\omega t} / (1 + i2Q\Delta\omega/\omega)$.

One possible implementation of this method to achieve such step current relationship is to phase lock I_1 and I_2 and choose the prepulse width $T = n\pi/\Delta\omega$, with n equal to an integer. Note that this method also applies to a cavity that is not detuned, i.e., with $\Delta\omega = 0$, where $I_1 = I_2 e^{(t_1 - T)/\tau} e^{-i\omega t_1} / (1 - e^{-T/\tau})$.

In the limit of zero pulse interval as $t_1 \rightarrow T$, such that $I_1 = I_2 e^{-i\omega T} / (1 - e^{-i\Delta\omega T} e^{-T/\tau})$, this profile will reduce to a two-step function. One can modulate the amplitude as shown in Fig. 13(a), or phase as shown in Fig. 14(a) of the first step I_1 relative to the following step I_2 . For the first case, one can phase lock I_1 and I_2 and choose the step width $T = 2n\pi/\omega$ and detuning $\Delta\omega = \omega/m$ with m and n

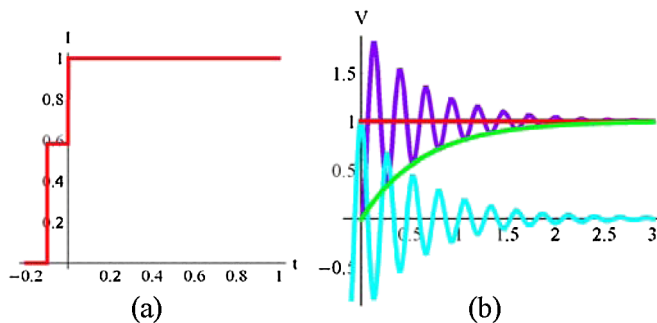


FIG. 13. (Color) Two-step functions. (a) Current profile. (b) The reduced filling time by cancellation of the two beating transients. The cyan curve is the voltage induced by the first step-pulse, the purple curve is induced by the second one, the red curve is the final voltage by summing two beating transients, and the green curve is the standard filling time curve for a single step pulse.

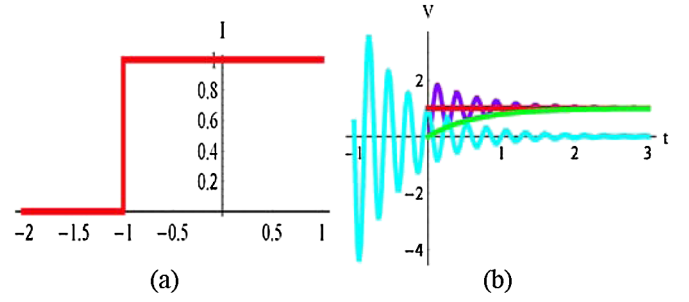


FIG. 14. (Color) Phase shift method. (a) Current profile. (b) The reduced filling time by cancellation of the two beating transients. The cyan curve is the voltage induced by the first step-pulse, the purple curve is induced by the second one, the red curve is the final voltage by summing two beating transients, and the green curve is the standard filling time curve for a single step pulse.

integers, such that the first and second currents are related by $I_1 = I_2 / (1 \pm e^{-T/\tau})$. The consequence of transient suppression is shown in Fig. 13(b).

As to the second case, one can choose $e^{-T/\tau} = 2 \cos \Delta\omega T$ with the constraint $\Delta\omega T > \pi/6$, such that $I_1 = I_2 e^{i(2\Delta\omega - \omega)T}$ with the phase flip equal to $(2\Delta\omega - \omega)T$, as shown in Fig. 14(b). Note that the phase flip case only works in the detuned cavity.

In conclusion, by modifying the beam profile in phase or amplitude, the effective beam filling time can be substantially shortened for the detuned acceleration structure. For the driven resonance cavity, the frequency shift due to the beam loading is a nonlinear effect that should be included in the model. Details of experimental implementation are beyond the scope of this paper.

One can see that in general it only takes only a time $\pi/\Delta\omega$ to fill the cavity instead of the nominal cavity filling time $\tau = 2Q/\omega_0$ by modifying the current pulse profile. For the detuned cavities as discussed in this paper, $Q\Delta\omega/\omega$ is in the order of several tens, hence the filling time can be shortened at least by a factor of 10.

- [1] S. V. Kuzikov and M. E. Plotkin, Joint 32nd International Conference on Infrared and Millimeter Waves, 2007 and the 2007 15th International Conference on Terahertz Electronics, pp. 797–798 [<http://ieeexplore.ieee.org/stamp/stamp.jsp?tp=&number=4516736&isonumber=4516365>]; S. Kazakov, S. V. Kuzikov, and J. L. Hirshfield, “Multimode, Multi-Frequency Two-Beam Accelerating Structure,” High-Gradient Collaboration Workshop, 2008 (unpublished).
- [2] S. V. Kuzikov and J. L. Hirshfield, in *Proceedings of the 23rd Particle Accelerator Conference, Vancouver, Canada, 2009* (IEEE, Piscataway, NJ, 2009).
- [3] S. V. Kuzikov, S. Yu. Kazakov, J. L. Hirshfield, M. E. Plotkin, A. A. Vikharev, and V. P. Yakovlev, CLIC Workshop, 2009 [<http://indico.cern.ch/sessionDisplay.py?sessionId=7&slotId=0&confId=45580#2009-10-14>].

- [4] A. Sessler and G. Westenskow, in *Handbook of Accelerator Physics and Engineering*, edited by A. W. Chao and M. Tigner (World Scientific, New Jersey, 2002), pp. 46–48.
- [5] H. Braun *et al.*, *CLIC 2008 Parameters*, CLIC-Note-764. See <http://cdsweb.cern.ch/record/1132079/files/CERN-OPEN-2008-021.pdf>.
- [6] E. Chojnacki, W. Gai, P. Schoessow, and J. Simpson, in *Proceedings of the IEEE 1991 Particle Accelerator Conference*, APS Beams Physics (IEEE, Piscataway, NJ, 1991), Vol. 5, pp. 2557–2559.
- [7] M. E. Conde, W. Gai, R. Konecny, J. Power, P. Schoessow, and P. Zou, in *Advanced Accelerator Concepts: Eighth Workshop*, edited by W. Lawson, C. Bellamy, and D. F. Brosius, AIP Conf. Proc. No. 472 (AIP, New York, 1998), pp. 626–634.
- [8] G. V. Sotnikov, T. C. Marshall, S. V. Shchelkunov, A. Didenko, and J. L. Hirshfield, *13th Advanced Accelerator Concepts Workshop (AAC2008)*, AIP Conf. Proc. No. 1086 (AIP, New York, 2009), pp. 415–420.
- [9] G. V. Sotnikov, T. C. Marshall, and J. L. Hirshfield, *Phys. Rev. ST Accel. Beams* **12**, 061302 (2009).
- [10] P. B. Wilson, *High Energy Electron Linacs: Applications to Storage Ring RF Systems and Linear Colliders*, AIP Conf. Proc. No. 87 (AIP, New York, 1982), pp. 550–563.
- [11] S. V. Kuzikov, S. Yu. Kazakov, M. E. Plotkin, and J. L. Hirshfield, in *Proceedings of the 11th European Particle Accelerator Conference, Genoa, 2008* (EPS-AG, Genoa, Italy, 2008), p. 2806, WEPP133 (2008).
- [12] S. Yu. Kazakov, S. V. Kuzikov, V. P. Yakovlev, and J. L. Hirshfield, in *Advanced Accelerator Concepts: 13th Workshop*, edited by C. B. Schroeder, W. Leemans, and E. Esarey, AIP Conf. Proc. No. 1086 (AIP, New York, 2009), Vol. 1086, pp. 439–444.
- [13] S. V. Kuzikov, S. Yu. Kazakov, Y. Jiang, and J. L. Hirshfield, *Phys. Rev. Lett.* **104**, 214801 (2010).